Hindawi
Mobile Information Systems
Volume 2017, Article ID 8198017, 15 pages
https://doi.org/10.1155/2017/8198017

Research Article

DIANA: A Machine Learning Mechanism for Adjusting the TDD Uplink-Downlink Configuration in XG-PON-LTE Systems

Panagiotis Sarigiannidis,[1] Antonios Sarigiannidis,[2] Ioannis Moscholios,[3] and Piotr Zwierzykowski[4]

[1]*Department of Informatics and Telecommunications Engineering, University of Western Macedonia, 501 00 Kozani, Greece*
[2]*Department of Economics, Democritus University of Thrace, University Campus, 691 00 Komotini, Greece*
[3]*Department of Informatics and Telecommunications, University of Peloponnese, 221 00 Tripoli, Greece*
[4]*Faculty of Electronics and Telecommunications, Poznań University of Technology, 60-965 Poznań, Poland*

Correspondence should be addressed to Panagiotis Sarigiannidis; psarigiannidis@uowm.gr

Received 22 February 2017; Revised 15 May 2017; Accepted 31 May 2017; Published 19 July 2017

Academic Editor: Massimo Condoluci

Modern broadband hybrid optical-wireless access networks have gained the attention of academia and industry due to their strategic advantages (cost-efficiency, huge bandwidth, flexibility, and mobility). At the same time, the proliferation of Software Defined Networking (SDN) enables the efficient reconfiguration of the underlying network components dynamically using SDN controllers. Hence, effective traffic-aware schemes are feasible in dynamically determining suitable configuration parameters for advancing the network performance. To this end, a novel machine learning mechanism is proposed for an SDN-enabled hybrid optical-wireless network. The proposed architecture consists of a 10-gigabit-capable passive optical network (XG-PON) in the network backhaul and multiple Long Term Evolution (LTE) radio access networks in the fronthaul. The proposed mechanism receives traffic-aware knowledge from the SDN controllers and applies an adjustment on the uplink-downlink configuration in the LTE radio communication. This traffic-aware mechanism is capable of determining the most suitable configuration based on the traffic dynamics in the whole hybrid network. The introduced scheme is evaluated in a realistic environment using real traffic traces such as Voice over IP (VoIP), real-time video, and streaming video. According to the obtained numerical results, the proposed mechanism offers significant improvements in the network performance in terms of latency and jitter.

1. Introduction

Modern telecommunication networks become increasingly complicated with various features and potentials. Their ambition is to provide end-users with ubiquitous access to advanced services and applications at a high-efficiency and high-quality level in a cost-efficient manner, any time, any place. Academia, industry, and emerging communities, that is, the 5th Generation (5G) Infrastructure Public Private Partnership (5G-PPP), promote the integration of the mobile and wireless with the wired and optical communications, given licensed and unlicensed spectrum features, while supporting the ubiquitous communication access to the last (or first) mile. Still, the access network domain, defined as the domain between the central office (CO) and the end-user connection points (e.g., home, curve, or building), remains the most arduous bottleneck in modern telecommunication networks. The ambitious challenge of upgrading the old copper-based infrastructure with modern optical networking components is still open. Even though during the last decade the capacity of core networks has experienced significant growth to meet the increasing bandwidth requirements, access networks constitute one of the trickiest puzzles [1].

Modern access networks are in front of three main challenges: (a) they have to be advanced in programmable components, (b) they have to support virtualization, and (c) they have to support high bandwidth to meet the latest user requirements. Software Defined Networking (SDN) technology seems promising to provide efficient solutions for the first challenge through a novel design principle that emerges to separate the control and the data plane functions. In essence, SDN enables the network programmability through

which the dynamic initialization, control, manipulation, and management in the access network are feasible [2]. Network Function Virtualization (NFV) employs standard IT virtualization technology to consolidate multiple network equipment types onto industry standard high volume servers, switches, and storage devices [3]. As a result, flexible network architectures, which are capable of adapting different vertical adaptation requirements, are feasible by industry players and operators [4, 5]. Lastly, demanding applications such as Voice over IP (VoIP), Video on Demand (VoD), High-Definition Television (HDTV), and online gaming entail a high-capacity network infrastructure that would allow mobility, flexibility, and Quality of Service (QoS) provisioning. In addition, the user's connectivity should be independent of the user's location.

Hybrid optical-wireless convergence constitutes a viable solution for addressing the bandwidth needs of the modern demanding applications and services. Hybrid optical-wireless networks integrate (a) broadband wireless solutions that are able to support multiple, and even mobile, end-users, such as Worldwide Interoperability for Microwave Access (WiMAX), third generation partnership project (3GPP), Long-Term Evolution (LTE), and Wireless Fidelity (Wi-Fi), for example, legacy IEEE 802.11, in a mesh environment and (b) optical technologies that bring huge bandwidth, however, in specific, fixed, and predefined optical paths, such as the passive optical network (PON) technology [6].

In this work, a hybrid optical-wireless architecture is considered which is enhanced with SDN controllers that govern the optical and wireless parts of the underlying infrastructure. The optical backhaul is designed in line with the 10-gigabit-capable passive optical network (XG-PON) system supporting up to 10 Gb/s downstream rate. The Optical Network Units (ONUs), which realize the connection interface of the PON to the final user, are enhanced with an evolved Node B (eNB) that is compatible with LTE Release 10. The integration of the ONU and the eNB is in line with the independent architecture concept [7]. This concept implies that both devices are connected independently, for example, by using a single cable. Hence, the bridging of the two domains (optical and wireless) is simple and flexible, needing no additional hardware. What this paper proposes is a novel machine learning mechanism that adjusts the uplink-downlink configuration based on the traffic conditions in the hybrid network. The SDN controllers provide the traffic status in terms of requested bits in both directions, that is, in the downlink (from the Optical Line Terminal (OLT) to the end-users) and in the uplink (from the end-users to the OLT) directions [8]. Next, the uplink-downlink ratio is manipulated in order to maximize the bandwidth allocation efficiency, given that the LTE cell operates under the Time Division Duplex (TDD) technique. To this end, a probabilistic-oriented learning process is introduced, entitled as Downlink to Uplink Ratio Determination (DIANA), which is able to effectively adjust the TDD configuration that governs the uplink-downlink offered bits ratio. According to the standard, seven TDD configuration options exist for defining the 10 ms LTE frame. The proposed framework succeeds in suitably changing this configuration in a periodic fashion by sensing the traffic changes in the network based on the SDN controller knowledge. Numerical results indicate the improvements of the proposed framework when applied in multiple channel scenarios in terms of latency and jitter. The results have been obtained by using real traffic traces in both downlink and uplink directions of the hybrid network.

The remainder of the paper is organized as follows. Section 2 presents the motivation behind this paper and the detailed contributions. Section 3 reviews research efforts in integrating optical and wireless technologies. Section 4 describes the proposed hybrid optical-wireless architecture. In Section 5, the proposed mechanism is presented in detail. Section 6 includes the performance evaluation of the proposed scheme in multiple simulation experiments. Various numerical results are presented and discussed. Finally, Section 7 concludes the paper and discusses future extensions.

2. Motivation and Contributions

Hybrid optical-wireless paradigms could leverage the advantages of optical and wireless technologies. Optical technology offers huge bandwidth and, in case of PONs, a cost-effective solution for creating a lightpath in the access domain. On the other hand, 4G technologies, such as LTE and LTE Advanced (LTE-A), exhibit high-speed wireless communication for mobile phones and advanced user terminals (laptops, tablets, and smartphones). The motivation behind this paper lies in the efficient convergence of these two different technologies in a way that will enable all supported cognitive features. For instance, LTE TDD framing allows an adjustable configuration of the uplink-downlink configuration. This is a feature that remains underutilized. In the light of the aforementioned remarks, the key contributions of this paper are summarized as follows:

(i) An effective optical-wireless access architecture is investigated, where the optical domain is controlled by an SDN-enabled XG-PON and the wireless connection fronthaul is based on the LTE technology. The hybrid ONU-eNB is governed by SDN controllers that are able to record the traffic conditions in the whole network.

(ii) A novel machine learning mechanism is proposed which is capable of effectively adjusting the uplink-downlink configuration of the LTE frame based on traffic dynamics.

(iii) An efficient probabilistic-based selection technique is presented which is able to adequately determine the most suitable configuration option for the forthcoming LTE TDD frame.

3. Related Work

The integration of optical and wireless technologies is also known as Fiber-Wireless (FiWi) architecture. Two main categories of FiWi architectures can be found in the literature: (a) Radio over Fiber (RoF), which encloses integration in the physical (PHY) layer, and (b) Radio and Fiber (R&F), which

includes separated optical and wireless domains in a bridged hybrid network. With the demonstration of the simultaneous modulation and transmission of a radio-frequency (RF) signal and a baseband (BB) signal, the challenge of transmitting both RF and BB signals on a single wavelength over a single fiber in a cost-effective way with acceptable performance has been addressed [9, 10]. To this end, Cloud Radio Access Network (C-RAN) emerges as a new paradigm capable of supporting efficient RoF solutions. It was proposed by many operators (e.g., IBM, Intel, Huawei, and ZTE) which features centralized processing, collaborative radio, real-time cloud computing, and power efficient infrastructure [11]. Its hybrid nature lies in its architecture: a central domain collects all computational resources stemming from all base station (BS). The collected radio-frequency signals are transmitted through the cloud by an optical network infrastructure. The rationale behind this integration of wireless and optical domains is to reduce the capital expenditures and the operating costs of the underlying infrastructure while providing advanced and even virtualized services and application to final users. On the other hand, R&F consists of hybrid wireless-optical architectures sharing a common characteristic: both domains are designed and deployed discretely by keeping their subtle features untouched. Usually, the optical domain governs the backhaul of the hybrid network, while the edges are equipped with wireless access interfaces. Different MAC protocols are used in each domain. This means that the optical and wireless media are handled by separate MAC controllers. R&F architecture may be formed in two different platforms based on the service provisioning orientation [6]. The first form is called hybrid optical-wireless mesh networking, where multiple connected wireless nodes expand the network range on an ad hoc basis. The second form is called hybrid optical-wireless access networking, where a single wireless BS is directly connected to the optical domain, mostly, via the ONU.

The term hybrid Wireless-Optical Broadband-Access Network (WOBAN) has been widely used for describing access networks that are composed of several wireless routers and a number of gateways connected to the ONUs, and through the OLT, to the rest of the Internet [12]. The WOBAN paradigm is realized as a compelling combination of (a) reliability, robustness, and high capacity, stemming from the optical communication domain, and (b) flexibility, mobility, and cost savings, stemming from the wireless domain. The Cloud-Integrated WOBAN was proposed as an extension of WOBAN architecture, where a network infrastructure provides cloud services within the access network [13]. On the other hand, hybrid optical-wireless access networking allows the integration of PONs with various broadband wireless technologies such as WiMAX, LTE, and Wi-Fi. The main difference of the hybrid optical-wireless access networking with the WOBAN paradigm lies in the number of connection steps. WOBAN creates a routing network of multiple wireless connection points, while optical-wireless access networks create a one-step connection point to the PON domain via a wireless BS.

By integrating E-PON in the backhaul and WiMAX in the fronthaul, a promising architecture is formed. In [7] a simple E-PON-WiMAX architecture was proposed. The integrated network aims at providing a cost-effective connection to the end-users in the access domain. The authors in [14] introduced the use of sub-OLTs which are placed between the OLT and ONUs. The sub-OLTs play the role of the traditional OLTs. The idea behind using sub-OLTs has to do with extending the network coverage. E-PON and LTE technologies were combined in [15]. An LTE network consists of the Evolved Packet Core (EPC) and the eNB. The E-PON-LTE architecture constitutes a cost-effective access network, where the mobility features of LTE with the huge capacity of E-PON are integrated in a cost-effective network.

The WDM-PON capabilities were investigated in [16], where an optical unidirectional WDM ring was integrated with a Wi-Fi-based mesh network. The network backhaul consists of an optical WDM ring equipped with single-channel or multichannel PONs. The interconnection of PONs and various mesh networks is achieved by means of wireless gateways located in mesh coverage networks. Convergence of WDM-PONs with LTE technologies was presented in [17]. Each eNB is integrated with the corresponding ONU located at an optical ring, while the EPC is connected to the OLT. Thousands of subscribers are able to reach the network by connecting to the eNB. The authors in [18] demonstrated an integration of G-PON with WiMAX. The work was focused on studying the QoS provisioning with multiple service classes defined by the WiMAX standard. In addition, several multistage schemes have been proposed in the previous years. This category includes the possible extended combination of multiple technologies. For example, a three-level network is proposed in [19]. The first level constitutes a WDM-E-PON, where the OLT is able to schedule transmissions using any available wavelength channel.

A comprehensive comparison on different integrated architectures can be found in [6] in terms of (a) equipment cost, (b) implementation complexity, (c) network coverage, (d) application protocol, (e) scalability, and (f) survivability. The usage of WDM technology seems still not so mature. On the other hand, WiMAX has not met the same popularity as the LTE standard. E-PONs provide Ethernet-based communication, which is quite common in the access domain. However, Gigabit-based PONs have penetrated the market more effectively. Nevertheless, new standards emerged in the last years: the 10 Gbps Ethernet PON (10 G-E-PON), based on IEEE 802.3ah, and the XG-PON, based on ITU. Hence, new updated architectures are needed for providing efficient and cost-effective solutions to the access network domain.

Recently, the concept of multiple transmit and receive apertures was investigated in [20]. The authors utilized generalized orthogonal space-time block codes of any arbitrary order and subcarrier intensity modulation scheme for data transmission over gamma-gamma fading optical links. They analytically evaluated the diversity order and the coding gain of the proposed system with gamma-gamma atmospheric turbulence. Also, the authors in [21] put the emerging Internet of Things (IoT) into the discussion of Fiber-Wireless (FiWi) networks. A comprehensive survey of recent progress and ongoing research works in related fields was provided, including QoS provisioning, reliability,

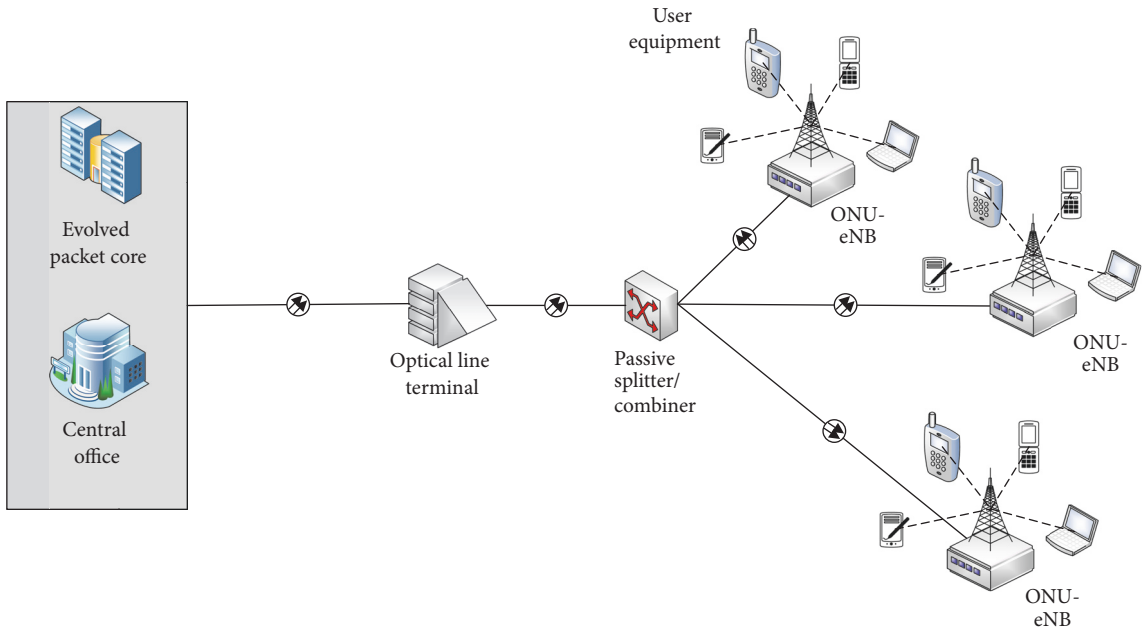

Figure 1: The XG-PON-LTE architecture.

energy saving, and case studies, indicating that hybrid optical-wireless networks still remain at the top of emerging technologies. New FiWi architectures are accompanied with novel protocols and bandwidth distribution schemes. In [22], a novel Medium Access Control (MAC) mechanism was proposed for the effective alleviation of highly loaded 60 GHz RoF networks. The protocol makes use of a memory buffer at the CO which offers reduction of the number of polling packets required. Also, various Dynamic Bandwidth Allocation (DBA) schemes are devised for managing the bandwidth scheduling in both domains. A prediction-aware DBA scheme for FiWi networks was introduced in [23], where a 10 G-E-PON is integrated with WiMAX radio access. A fair bandwidth distribution is applied based on the results of the underlying prediction mechanism. In [24], the convergence of optical and wireless technologies is studied in a different prospective. The authors use a weighted fairness provisioning technique, intending to alleviate the interdependence of the two domains, offering a fair and efficient bandwidth distribution to the mobile users. The work includes a weight determination mechanism by utilizing Lagrange multipliers. Simulation results indicate the capability of the proposed fair scheme in provisioning efficient and fair bandwidth distribution in generic hybrid optical-wireless networks. The concept of metaheuristics is also the topic of the work in [25]. The authors apply the well-known ant colony optimization method for optimizing the bandwidth report process of mobile users. Simulation results indicate significant improvements in terms of latency and network throughput.

In a nutshell, there is a plethora of hybrid architectures and bandwidth distribution schemes as well. However, there is a lack of integrating new standards such as XG-PON. In addition, all the aforementioned schemes, using either WiMAX or LTE, assume a stable uplink-downlink configuration. Thus, the bandwidth distribution becomes static and traffic-unaware. Given that mobile users generate unpredictable and bursty traffic, the need of adjusting the uplink-downlink configuration towards the maximization of the network performance becomes critical.

4. Architecture

The architecture of the proposed hybrid XG-PON-LTE scheme is presented in this section along with the underlying SDN controller which is responsible for handling user requests in both directions of the hybrid network.

4.1. Integration of Optical and Wireless Components. Figure 1 illustrates the proposed XG-PON-LTE architecture. On the left of the figure, the backhaul is defined between the CO and the ONU-eNB edges. This part is governed by the XG-PON system. The OLT is connected directly with the passive splitter/combiner via optical fiber. The passive splitter/combiner operates without needing external power. In the downlink direction, it divides the optical fiber to N ONU interfaces. In the upstream direction, it combines N optical fibers (stemming from the ONU interfaces) with a single optical fiber towards the OLT. It is clear that a lightpath is created between the CO and the ONU-eNBs, meaning that a cost-effective topology is realized which engages several merits such as low maintenance, protocol transparency, and low operation cost. The ONU-eNB constitutes a hybrid optical-wireless network entity capable of supporting two interfaces: (a) an optical interface that interconnects the ONU-eNB with the OLT and (b) a wireless interface that realizes an LTE radio access network. The EPC, which is the latest evolution of the 3GPP core network architecture, is located at the CO. Its architecture separates the user data (user plane) and the signaling (control plane) to make the scaling independent. Thus, the telecom providers and operators could handle the

channel and (cellular) network configurations easily. User equipment (UE) is defined as any kind of device that is used directly by an end-user to communicate with the e-NB. It can be a laptop, a cellular phone, a tablet, and so forth.

The huge capacity of the optical domain lies in the ability of XG-PON systems to support 10 Gbps in at least one direction. Two wavelengths are used, one for the upstream transmission at the 1270 nm and the other for the downstream transmission at the 1577 nm. The downstream transmission rate in XG-PON systems is 9.95328 Gbps [26]. Thus, 9.95328 Gbps is the nominal rate of the downstream direction. The OLT is continuously transmitting in the downstream direction, where fixed size downstream PHY frames are continuously sent to the ONUs (ONU-eNBs in our case). These downstream frames are periodically transmitted towards the ONU-eNBs every 125 μsec. As a result, $9.95328 \cdot 10^9 \cdot 125 \cdot 10^6 = 1244160$ bits = 155520 bytes are available in the downstream direction. A downstream frame is composed of, among others, the BWmap field. The BWmap is critical, since it is used by the OLT to inform the ONU-eNBs about the decided (upstream) transmission opportunities. The upstream transmission rate is 2.48832 Gbps (there is a symmetrical standard as well), while the upstream frame is 125 μsec long. Thus, 38880 bytes are available for upstream transmission opportunities. Alloc-IDs are the main user ports in the XG-PON. In our work, we consider that no users directly connected to the ONU ports exist. Hence, Alloc-IDs are represented by the UEs.

OLT is responsible for allocating guaranteed and non-guaranteed bandwidth to all Alloc-IDs. The amount of guaranteed bandwidth includes the fixed bandwidth and the assured bandwidth flows. There is also a maximum guaranteed bandwidth granted to each ONU-eNB.

4.2. SDN Controllers. As previously mentioned, SDN abstracts and separates the data forwarding plane from the control plane, allowing faster technological development in both data and control planes. SDN offers a simplified view of the underlying network infrastructure for the network control and monitoring applications through the abstraction of each independent network layer [2]. In this paper, the proposed architecture is enhanced with SDN controllers that provide the traffic status in terms of requested bits in both directions, that is, in the downlink (from the Optical Line Terminal (OLT) to the end-users) and in the uplink (from the end-users to the OLT) directions. The rationale behind the usage of SDN controllers lies in the advantages that SDN technology offers in terms of flexibility and adaptability. By enabling the SDN control down to the photonic level operation of optical communications allows for flexible adaptation of the photonic components supporting optical networking functionalities [27].

The operation of each ONU-eNB is monitored and governed by an equal number of SDN controllers (ONU-eNB SDN controllers). Another controller governs the OLT operation (OLT SDN controller). Figure 2 illustrates how the SDN controllers divide the underlying infrastructure into data and control planes. In essence, the SDN controllers are able to adjust a set of device configuration parameters. In the context of this work, we consider that each SDN controller that is attached to an ONU-eNB is able to adjust the TDD uplink-downlink configuration. Similarly, it is assumed that the OLT is manipulated by an SDN controller which is capable of monitoring the user requests in the uplink and the downlink directions. In particular, the traditional OLT is upgraded in an SDN-OLT that can be controlled using a Southbound Interface (SI), such as OpenFlow [28]. Also, the SDN concept of [29] is adopted, where the SDN controller leverages its broad view of the network to provide solutions to the joint bandwidth allocation network. To this end, efficient bandwidth allocation schemes can be applied with the aim of the underlying SDN controllers. To be more specific, the controller behind the SDN-OLT monitors the buffer occupancy (BufOcc) field of each upstream XG-PON transmission convergence (XGTC) burst. BufOcc is 3 bytes long and contains the total amount of the Service Data Unit (SDU) traffic, coming from the wireless radio interfaces. To this end, the SDN-OLT is aware of the upstream traffic of each ONU-eNB. At the same time, the SDN-OLT is equipped with a logical buffer that receives data coming from the backbone network and destined to the ONU-eNBs. Thus, the SDN controller is aware of the traffic requested in both directions. As a result, adaptive decisions regarding the bandwidth allocation process can be made in the control plane.

5. Machine Learning Mechanism

5.1. Background. A hybrid optical-wireless access network is considered. In the backhaul, an XG-PON infrastructure provides access to the backbone to end-users. In the fronthaul edges, ONU-eNBs consist of the connection points where the end-users are connected to the hybrid network through UEs. We assume that the hybrid network comprises N ONU-eNBs and a single OLT. In addition, the eNB part of the ONU-eNB is compliant with LTE Release 10 [30]. The notations used in the following modelling are summarized in "Notations" at the end of the paper.

LTE has been designed as a highly flexible radio access technology in order to support several system bandwidth configurations (from 1.4 MHz up to 20 MHz) [31]. In the uplink direction, the Single-Carrier Frequency Division Multiple Access (SC-FDMA) is used. The downlink direction utilizes the Orthogonal FDMA (OFDMA) technique. The subtle difference between the two techniques has to do with the way of allowing access to users. OFDMA can exploit subcarriers distributed inside the entire spectrum, whereas SC-FDMA can use only adjacent subcarriers. The rationale behind this difference lies in the usage of each technique. OFDMA was designed to provide LTE with high scalability, simple equalization, and high robustness. On the other hand, SC-FDMA is focused on keeping an energy-aware user access scheme, giving emphasis to the limited energy of the UE.

The LTE framing is quite flexible. Two types of frame structure are allowed depending on the defined resource management. If the resource management allows frequency duplexing, the Frequency Division Duplex (FDD) technique is adopted, where the two directions, that is, upstream and downstream, are carried in two frequencies and the

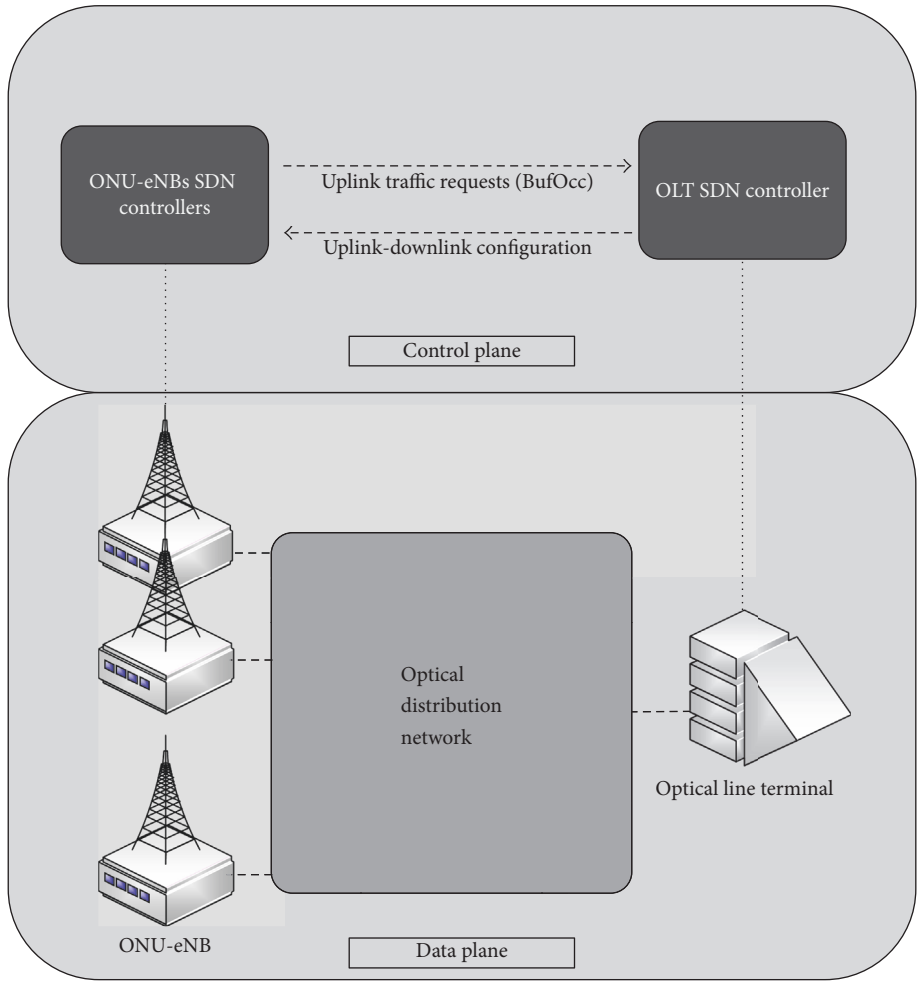

Figure 2: The operation of the SDN controllers as the data and the control planes are divided.

transmitting and receiving of data are simultaneous. Thus, the function of FDD techniques implies a symmetric use of the available bandwidth. On the other hand, TDD enables more flexible management of the available bandwidth. TDD technique emulates full duplex communication using a half-duplex link. Two consecutive half-frames are defined, with each one lasting 5 ms. As a result, flexible configurations are allowed in defining the relation of the downlink to the uplink transmission duration.

It is considered that the eNB interface of the ONU-eNB supports TDD as the main duplexing technique. Hence, the LTE frame has an overall length of 10 ms, while it consists of 10 subframes. Each subframe is further divided into two slots. The length of each subframe is 1 ms, while the length of each slot is 0.5 ms. The standard configuration set of defining the ratio between the downlink and the uplink directions is adopted, where a total of 7 uplink-downlink configurations exist. Keeping the first and the sixth subframes always dedicated to the downlink direction, the remaining eight subframes could be configured dynamically in line with the predefined 7 configuration options. It is worth mentioning that the first subframe is always dedicated to broadcast purposes, since the BS informs the connected UEs about the configuration parameters of the ongoing communication. This is the reason way any change that is related to the radio interface parameters should be broadcast in the beginning of each LTE frame. Table 1 outlines the available uplink-downlink configurations, starting from the first one and ending at the last one. "D" stands for a downlink subframe, while "U" stands for an uplink one. "S" denotes the special subframe which is used for guarding. When switching from downlink to uplink direction, there is a need for a special switching subframe. No special subframe is used when switching from uplink to downlink direction.

The set of the uplink-downlink configuration options is modelled as $C = \{c_0, c_1, \ldots, c_7\}$, where c_0 stands for the first uplink-to-downlink configuration option (0) and c_1 symbolizes the second (1) and so on. Given an applied configuration option, each frame encloses a specific amount of downlink and uplink bits for data delivery. Let $R = \{r_0, r_1, \ldots, r_7\}$ denote the downlink-to-uplink ratio in terms of offered bits. For example, r_0 stands for the downlink-to-uplink ratio in terms of bits when the first configuration option is in place (c_0).

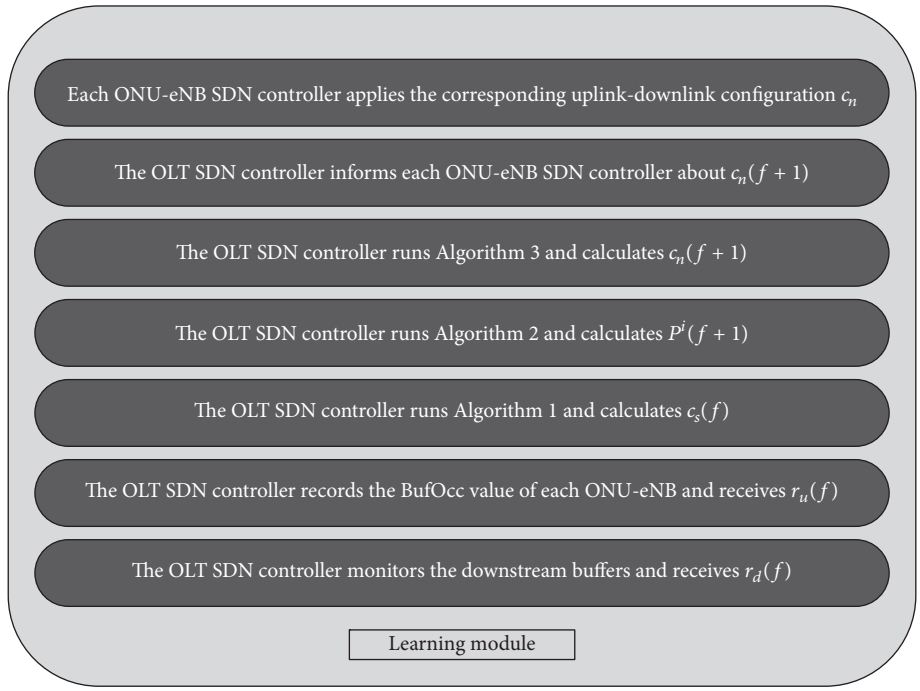

Figure 3: The learning module of DIANA in steps starting from the bottom and going to the top.

Table 1: Uplink-downlink configurations.

Uplink-downlink configuration	Subframes
0	D-S-U-U-U-D-S-U-U-U
1	D-S-U-U-D-D-S-U-U-D
2	D-S-U-D-D-D-S-U-D-D
3	D-S-U-U-U-D-D-D-D-D
4	D-S-U-U-D-D-D-D-D-D
5	D-S-U-D-D-D-D-D-D-D
6	D-S-U-U-U-D-S-U-U-D

In each fth LTE frame, assume that $r_d^i(f)$ and $r_u^i(f)$ denote the total requested bits in the downlink (from the ith ONU-eNB to the connected UEs) and the uplink (from the corresponding UEs to this ONU-eNB) directions, respectively.

5.2. Problem Formulation. The objective of the designed learning module is to adjust the uplink-downlink configuration based on the traffic conditions in ONU-eNBs. The decision is announced, using the first downlink subframe, in the beginning of each LTE frame, that is, for each 10 ms. In essence, the decision is made during the previous subframe, that is, within 1 ms, since the OLT SDN controller is aware of the downlink and uplink traffic requests. This is due to the fact that each ONU-eNB should make its decision on the following uplink-downlink configuration before starting the first subframe, where the UEs are informed about the status of the ongoing frame.

The OLT SDN controller records the ONU-eNB traffic requests in both directions and after processing the requested data and the feedback, perceived in the previous frame, makes a decision for the forthcoming LTE frame. The ONU-eNB SDN controllers communicate with the SDN-OLT using the ONU Management and Control Interface (OMCI), which in traditional PONs constitutes the core signaling mechanism between the ONUs and the OLT; thus each ONU-eNB is informed about the decided uplink-downlink configuration for the forthcoming LTE frame. In essence, the OLT SDN controller makes a decision regarding the TDD uplink-downlink configuration about the forthcoming LTE frame, for each ONU-eNB, and announces it to the ONU-eNB using the OMCI. Then, the ONU-eNB SDN controllers apply the new TDD uplink-downlink configuration in the underlying ONU-eNB devices.

5.3. Learning Module. The learning module aims at determining the most suitable uplink-downlink configuration for maximizing the network performance based on the ongoing traffic conditions in the hybrid optical-wireless network. Figure 3 shows the steps of the learning module starting from the bottom and going to the top. A probability vector is defined (each f LTE frame) for facilitating the decision-making of the OLT SDN controller as follows:

$$P^i(f) = \left\{p_0^i(f), p_1^i(f), \ldots, p_6^i(f)\right\}. \quad (1)$$

$P^i(f)$ includes 7 member probabilities in line with the total uplink-downlink configuration options. Thus, $p_0^i(f)$ stands for the first configuration option (c_0) and $p_1^i(f)$ stands for the second configuration option (c_1) and so on.

This probability vector implies how likely each configuration is to appear as the most suitable one. Note that each

Data: R, N
Result: $c_s^i(f)$
(1) **for** *each* f*th frame* **do**
(2) **for** *each* $i = 1, 2, \ldots, N$ *ONU-eNBs* **do**
(3) Record $r_d^i(f)$
(4) Record $r_u^i(f)$
(5) Set $r^i = r_d^i(f)/r_u^i(f)$
(6) Calculate $\arg\min_s\{|r^i - r_s|\}$
(7) $c_s^i(f)$ is extracted as feedback
(8) **end**
(9) **end**

Algorithm 1: Feedback determination.

probability is indexed by i which refers to the ONU-eNB those probabilities stand for. This is due to the fact that different traffic conditions may exist in each ONU-eNB. It is clear that the summation of all probabilities, for each ONU-eNB, is equal to unity:

$$\sum_{j=0}^{6} p_j^i(f) = 1. \quad (2)$$

Initially, the probability vector is initialized equally for all configurations:

$$p_j^i(f) = \frac{1}{7}, \quad \forall i, j,\ 1 \le i \le N,\ 0 \le j \le 6. \quad (3)$$

In the light of the aforementioned remarks, the objective of the OLT SDN controller is to estimate the most suitable uplink-downlink configuration, out of the C set, for the next LTE frame for each ONU-eNB. Obviously, this process entails a short-term estimation which is based on the traffic conditions in each ONU-eNB.

The definition of the feedback received by the OLT SDN controller in order to proceed with the selection of the most appropriate configuration option is crucial. At the end of the f LTE frame, the OLT SDN controller records the following metrics: $r_d^i(f)$ and $r_u^i(f)$. The feedback is formulated as the most suitable configuration for the last frame based on those metrics. Thus, the feedback expresses the most suitable configuration option for frame fth, denoted as $c_s^i(f)$. Algorithm 1 shows the feedback determination process. In each frame fth, it receives R and N and exports the feedback for the specific frame. It calculates the ratio of requested data bits in downlink to uplink direction ($r^i = r_d^i/r_u^i$). After that, it finds the most suitable r_s, $s = 0, 1, 2, \ldots, 6$, which is closer to the value of r^i. The whole process is repeated for each $i = 1, 2, \ldots, N$ ONU-eNB.

In Algorithm 2, the probability vector $P^i(f)$ is updated based on the feedback of frame f. Algorithm 2 illustrates the updating process. It receives the probability vector as defined in frame f ($P^i(f)$), the feedback as acquired from frame f ($c_s^i(f)$), the number of ONU-eNBs (N), and two convergence parameters (W and a). W controls the convergence speed of the learning process. a is adopted in order to prevent reaching zero probabilities. Usually, it receives a very small, fixed value (e.g., 104). The output of the algorithm is the probability vector of the next frame ($P^i(f+1)$). Given that the feedback indicates configuration s as the appropriate one for fth frame, all other configuration probabilities are slightly reduced (line (3)). The total decrease is denoted as S. In Algorithm 2 (line (5)), the configuration probability that is related to s is increased by S. In this way, the "winning" configuration is distinguished from the others, since it is selected as the appropriate one according to the ongoing traffic requests in each ONU-eNB.

5.4. Selection Process. Upon determining the most suitable configuration of frame fth and updating the probability vector, SDN controllers make their decision for the next frame $(f+1)$th for each ONU-eNB. Algorithm 3 is presented as the selection process of the uplink-downlink selected configuration for the next frame $(f+1)$th. The algorithm accepts the updated probability vector ($P^i(f+1)$) and the number of ONU-eNBs (N) and extracts the selected configuration $c_n^i(f+1)$. In essence, the algorithm selects the configuration that is related to the maximum probability (line (3)). $c_n^i(f)$ will be the uplink-downlink configuration for the next LTE frame.

Figure 4 depicts the operation, the interconnection, and the products of the three algorithms presented. In essence, the three algorithms are the core of the learning procedure. The OLT SDN controller performs these algorithms on one by one basis in order to define the necessary building blocks for determining the most suitable uplink-downlink configuration for each ONU-eNB for the next frame.

5.5. Numerical Example. In order for the reader to better comprehend the aforementioned model, hereafter we provide a numerical example. Assume that five UEs are connected to the second ONU-eNB ($i = 2$). At the end of frame $f = 100$, the probability vector P^2 has been formed as follows:

$$P^2(100) = \{0.1, 0.25, 0.2, 0.25, 0.05, 0.05, 0.1\}. \quad (4)$$

The SDN controller records the values of $r_d^2(100)$ and $r_u^2(100)$. Assume that $r_d^2(100) = 25000$ bits and $r_u^2(100) = 18000$ bits. As a result, it holds that $r^2 = 25000/18000 = 1.38$. Algorithm 1 will run accordingly. Assuming that $R = \{0.97, 1.34, 2.69, 2.00, 2.88, 5.76, 1.12\}$, Algorithm 1 receives R and calculates the suitable configuration which is 1, since the difference $|1.48 - 1.34|$ is the minimum difference between any other members of the R set. In the following, Algorithm 2 updates the probability vector. It receives the current probability vector ($P^2(100)$) and the suitable configuration ($c_1^2(100)$) and exports the updated probability vector ($P^2(101)$). In the operation of Algorithm 2, consider $W = 10^{-2}$ and $a = 10^{-4}$:

$$P^2(101) = \{0.09, 0.29, 0.19, 0.24, 0.04, 0.04, 0.09\} \quad (5)$$

Upon determining the updated probability vector, the selection process takes place in order to find the selected configuration for the next frame $f = 101$. Algorithm 3 extracts 1

Data: $P^i(f), c_s^i(f), N, W, a$
Result: $P^i(f+1)$
(1) **for** *each* f*th frame* **do**
(2) **for** *each* $i = 1, 2, \ldots, N$ *ONU-eNBs* **do**
(3) Set $p_j^i(f+1) = p_j^i(f) - W(p_j^i(f) - a),\ \forall j,\ 0 \le j \le 6,\ j \ne s$
(4) Set $S = W \cdot \sum_{q=0, q\ne s}^{6}(p_q^i(f) - a)$
(5) Set $p_s^i(f+1) = p_s^i(f) + S$
(6) **end**
(7) **end**

Algorithm 2: Probability vector update.

Data: $P^i(f+1), N$
Result: $c_n^i(f+1)$
(1) **for** *each* f*th frame* **do**
(2) **for** *each* $i = 1, 2, \ldots, N$ *ONU-eNBs* **do**
(3) Calculate $\arg\max_n\{p_n^i(f+1)\}$
(4) $c_n^i(f+1)$ is extracted as the selected configuration for the $(f+1)$th frame
(5) **end**
(6) **end**

Algorithm 3: Selection process.

as the most suitable configuration, since it has the maximum probability. Note that, during the selection process, the values of $r_d^2(101)$ and $r_u^2(101)$ are still unknown, since the forthcoming frame is not started yet. The extracted configuration is applied to the forthcoming frame $f = 101$, which means that the distribution of the subframes will be D-S-U-U-D-D-S-U-U-D.

6. Performance Evaluation

This section is devoted to the performance evaluation of DIANA, including the evaluation environment and the obtained numerical results.

6.1. Evaluation Environment. A hybrid optical-wireless XG-PON-LTE-A network was implemented using the LTE system Toolbox in Matlab [32]. The optical backhaul consisted of a single OLT and $N = 8$ ONU-eNBs. The interconnection among the OLT and the ONU-eNBs followed a tree topology. No users were considered in the optical part of the hybrid network. As a result, the traffic was generated by UEs exclusively. The downstream and the upstream transmission rates in the XG-PON part were set in line with the ITU-T G987.3 specifications, that is, 9.95328 and 2.48832 Gbps, respectively. In line with the standard, the OLT periodically broadcasts a downstream frame each 125 μsec to all ONU-eNBs. The OLT, the ONU-eNBs, and the UEs maintain quite large buffers, for example, 1 GB each; hence, no packet drop was considered due to buffer overflow. The distance between the OLT and the ONU-eNBs was uniformly selected within [20, 60] Km. This results in propagation delay between [1, 3] msec given a propagation speed of 200000 Km/s. The ONU-eNB response time was set as 35 μsec for processing the downstream frame stemming from the OLT. Also, the OLT exchanged a uniformly distributed number of [1, 10] PLOAM messages with the connected ONU-eNBs through the PLOAM channel.

A guard time equal to 64 bits was kept within upstream allocation in the XG-PON upstream direction. The fixed and the assured bandwidth values were set as 100 and 200 bytes per 125 μsec. The upper limit of guaranteed bandwidth was 500 bytes per 125 μsec in total. The Pure Status Reporting (PSR) scheme was adopted, where each ONU-eNB reports its (uplink) queue occupancy to the OLT using the BufOcc field. Regarding the learning process, it holds that $W = 10^{-2}$ and $a = 10^{-4}$.

The frame structure in the LTE radio access network, which holds for each ONU-eNB, is organized in downlink and uplink transmissions using type 2 which is applicable to TDD. The duration of the frame was 10 ms. Each frame enclosed 10 subframes of 1 length each. The default uplink-downlink configuration was 1 which defines the following subframe number: D, S, U, U, D, D, S, U, U, D. No interference between UEs was considered.

Two scenarios were considered regarding the reference channel options in downlink and uplink directions. In the first scenario, the downlink reference channel was set to 16 QAM and "1/2." Table 2 summarizes the downlink reference channel options. At the same time, the uplink reference channel in the first scenario was considered as 16 QAM and "3/4." Table 3 depicts the detailed uplink channel options for scenario 1.

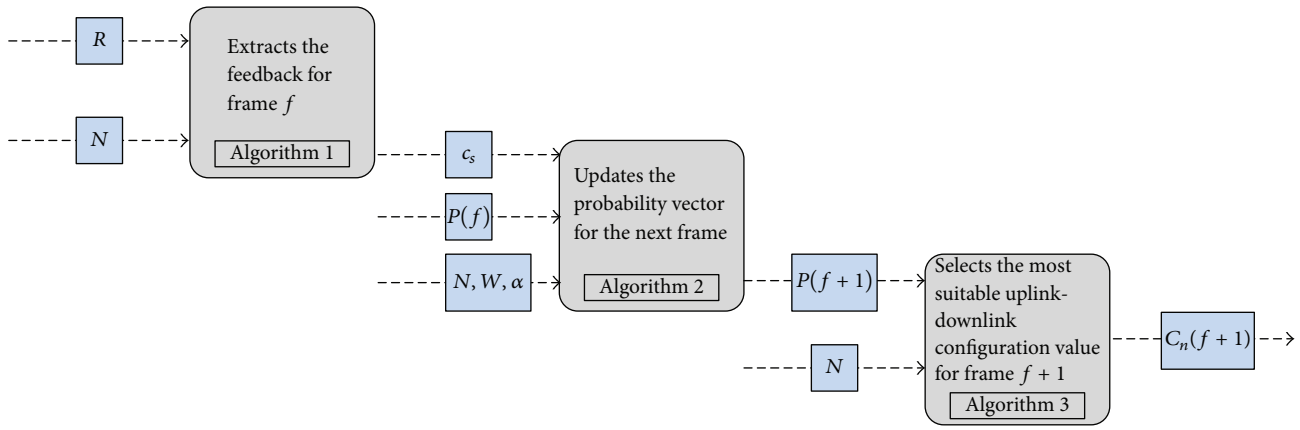

Figure 4: The operation, the interconnection, and the output of each algorithm in the context of the learning module.

Table 2: Scenario 1: downlink reference channel options.

Channel bandwidth	10 MHz
Allocated resource blocks	50
Modulation	16 QAM
Target coding rate	1/2

Table 3: Scenario 1: uplink reference channel options.

Channel bandwidth	10 MHz
Allocated resource blocks	1
Modulation	QPSK
Target coding rate	1/3

Table 4: Scenario 2: uplink reference channel options.

Channel bandwidth	10 MHz
Allocated resource blocks	1
Modulation	16 QAM
Target coding rate	3/4

Table 4 provides the detailed channel options for scenario 2. Note that in scenario 2 the same downlink reference channel features were used as depicted in Table 2.

6.2. Traffic Parameters. Real traffic traces were used for generating traffic in both directions in the hybrid optical-wireless network. This traffic belongs to three real applications, namely, (a) Voice over IP (VoIP) application, (b) real-time video application, and (c) streaming video application. These traffic streams have been recorded in an actual LTE infrastructure, where Skype (without video) was used for producing the VoIP application, Skype (teleconference) was used for producing the real-time video, and YouTube was used for producing the streaming video. For the following simulation scenarios, we consider a dynamic mixture of generated traffic, where each UE has a probability of 80% of initializing a VoIP session upon its connection establishment with the corresponding ONU-eNB. This means that a UE might not use a VoIP session at all, while other UEs might use a VoIP session. In this way, the combination of the traffic generated in the UEs becomes more dynamic and thus more realistic. To this end, it is challenging to investigate how DIANA will address traffic dynamics in real time. The VoIP session generates about 5.5 and 53 Kbps in the upstream and the downstream directions, respectively. In addition, each UE may initialize a real-video application with probability equal to 70%. A real-video application generates about 5 Kbps and 3.6 Mbps in the upstream and the downstream directions, respectively. Lastly, a streaming video session may be initialized by a UE with probability equal to 60%. The generated traffic by the streaming video application is about 5.8 Kbps and 11.6 Mbps in the upstream and the downstream directions, respectively.

6.3. Performance Metrics. The numerical results of assessing two schemes are presented. For comparison reasons, DIANA is evaluated in contrast to a standard-compliant scheme that keeps the default uplink-downlink configuration (1) stable for the whole experiment. DIANA and the static scheme are compared in terms of upstream latency and downstream latency, VoIP upstream latency and VoIP downstream latency, video upstream latency and video downstream latency, and VoIP jitter. Latency was measured considering an end-to-end communication between the OLT and the UEs (downlink) and vice versa (uplink). It should be stressed that a first-in, first-out policy was followed in all scheduling tasks (e.g., in forwarding data packets from the OLT queue for downstream transmission) for both schemes under comparison.

6.4. Numerical Results. This subsection presents the numerical results obtained by assessing DIANA and the static scheme for both scenarios. For all experiments, the number of UEs is changed from 10 to 30 per ONU-eNB, while keeping fixed the number of ONU-eNBs in the hybrid network. Each experiment lasts for 10 min. Initially, the network is populated with 1 (in case of 10 UEs) UE per ONU-eNB. A new UE is connected to each ONU-eNB for each further minute. For example, when x-axis is 10, the network begins with a UE per ONU-eNB during the first minute, it continues

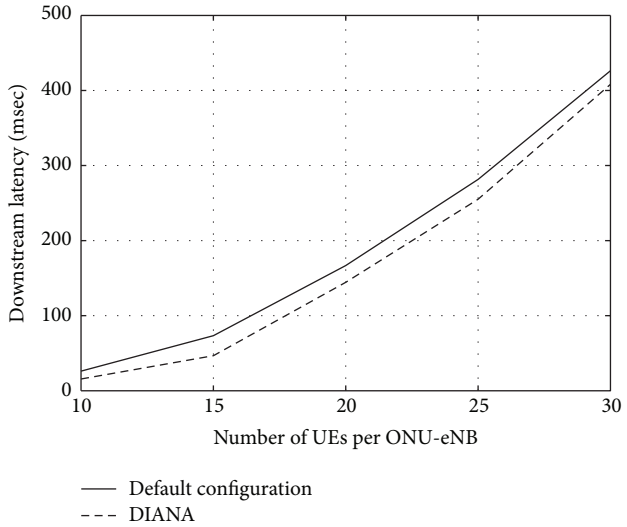

Figure 5: Scenario 1: average downstream latency.

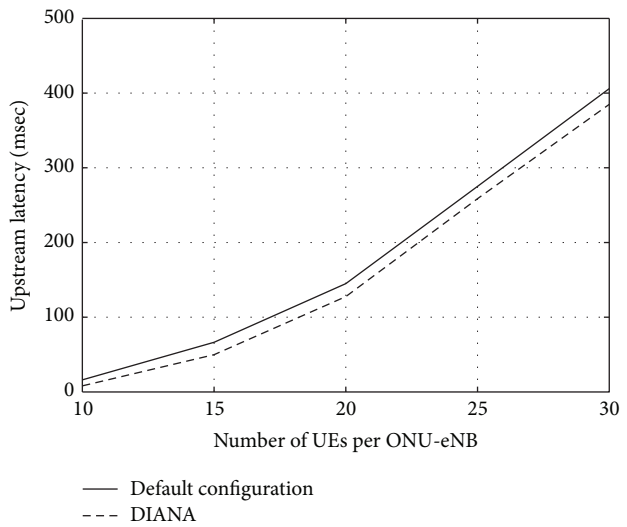

Figure 6: Scenario 1: average upstream latency.

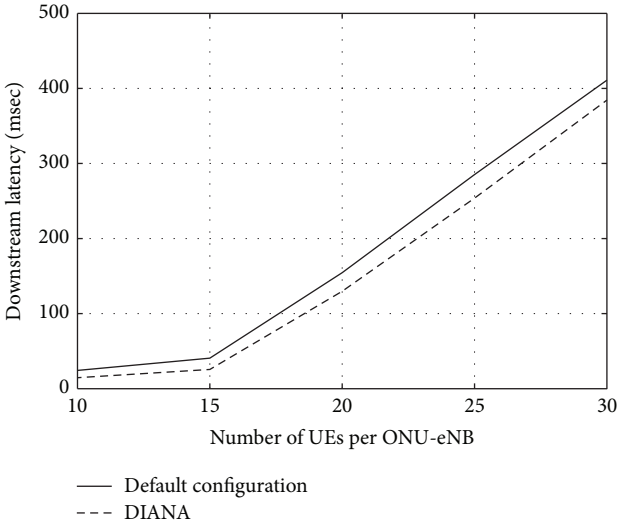

Figure 7: Scenario 2: average downstream latency.

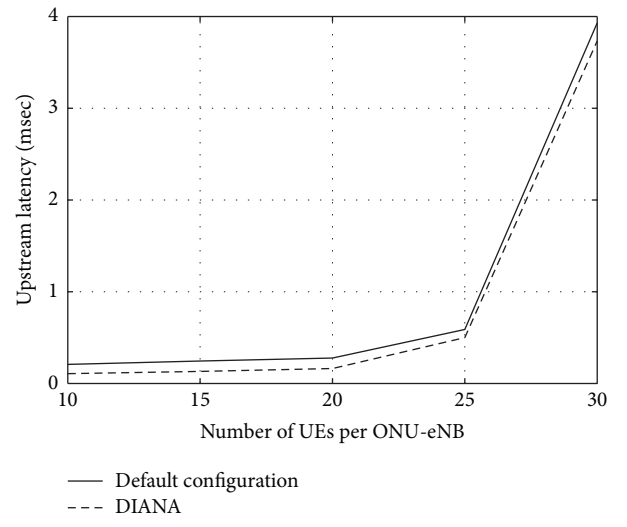

Figure 8: Scenario 2: average upstream latency.

with one more UE per ONU-eNB in the second minute, and it encloses 20 UEs per ONU-eNB in the final minute. In other words, the mobile user population is dynamic in order to measure the performance of both schemes when the traffic dynamics are always changed. In essence, for each x-axis value, the number of UEs is dynamically changed from $x - 9$ to $x + 10$, where x stands for the x-axis value.

Figures 5 and 6 show the average latency in downlink and uplink directions, respectively, in scenario 1. The dashed curve represents DIANA, while the black solid curve shows the performance of the static scheme. Figures 7 and 8 illustrate the average latency in downlink and uplink directions, respectively, in scenario 2. Four main aspects can be extracted by observing these four figures. First, the latency is increased as new UEs enter the hybrid network in both directions. This is a phenomenon that is repeated in all the aforementioned figures (Figures 5–8), since new UEs bring more traffic requests in both directions. Second, DIANA is able to reduce the latency by almost 40% at average in scenario 1 and by almost 30% at average in scenario 2. DIANA keeps a better performance in all scenarios for both directions. This is attached to the learning-aware mechanism of DIANA which has been proven to be beneficial to the network performance. It is capable of selecting suitable uplink-downlink configuration based on traffic conditions. On the other hand, the static scheme follows as fixed configuration option that keeps equal ratio between downlink and uplink directions. However, as new UEs establish connections, the traffic dynamics are changed. For instance, some UEs may request more downlink than uplink data. As a result, the default configuration is inefficient to meet the users' requirements. For example, in many cases, during simulations, we observed that uplink transmission opportunities were underutilized, while downlink streams had to wait for bandwidth to be available. Third,

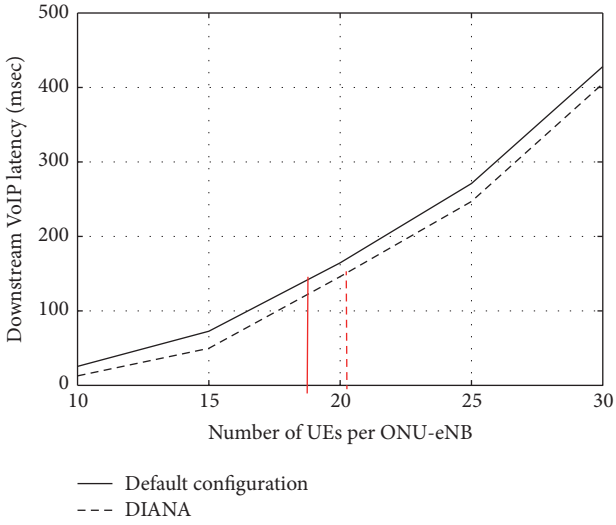

Figure 9: Scenario 1: VoIP downstream latency.

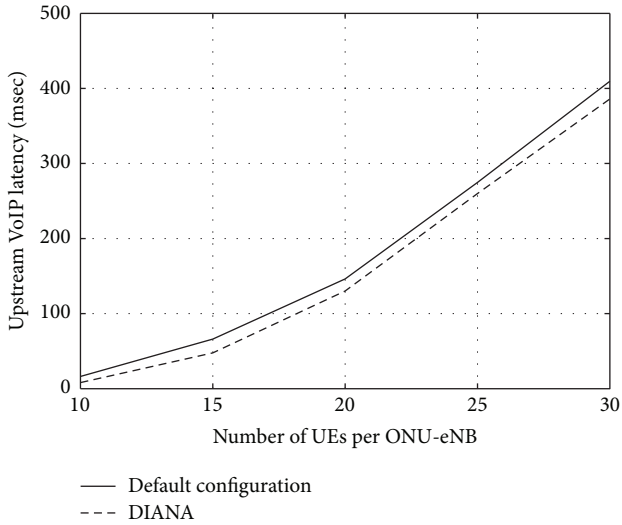

Figure 10: Scenario 1: VoIP upstream latency.

the uplink latency in scenario 2 is much reduced compared to the first scenario. This fact was expected, since the channel parameters in the second scenario allow offering more bits in the uplink direction; thus the uplink throughput was much higher. Lastly, the latency observed in the downlink and uplink directions in the first scenario seems to have a similar behaviour. This phenomenon is the result of two facts. First, the modulation schemes are different in each direction, that is, 16 QAM for the downlink direction and QPSK for the uplink direction. Second, the traffic load in the downlink direction is much more than that in the uplink direction. As a result, more traffic load is carried in the downlink direction compared to the uplink one; however, the uplink rate is limited by the less efficient modulation scheme. Thus, an unexpected similarity is observed, where the acquired latencies are similar in both directions. On the contrary, the observed latency in scenario 2 is totally different when the two directions are compared. By applying 16 QAM in the uplink direction, the recorded latency is quite reduced. For instance, the uplink latency is kept under 1 msec when the number of UEs is up to 25, while the observed downlink latency is almost ×100 higher.

In the following, the performance of the two schemes is investigated subject to the VoIP session. VoIP results from scenario 1 regarding downlink and uplink directions are drawn in Figures 9 and 10, respectively. Accordingly, Figures 11 and 12 illustrate the VoIP results from scenario 2. VoIP service is a crucial application, since it entails strict QoS requirements. Any violation in VoIP service requirements, that is, latency higher than 150 msec, could harm the quality of the communication. To this end, red lines mark the VoIP requirements in terms of latency in Figures 9 and 11. While the static scheme can handle 18 UEs, DIANA is able to support about 21 UEs based on results of scenario 1. Similarly, in scenario 2, DIANA offers 2 more UEs, meaning that more users may be served using the same resource by adequately adjusting the uplink-downlink configuration based on network dynamics.

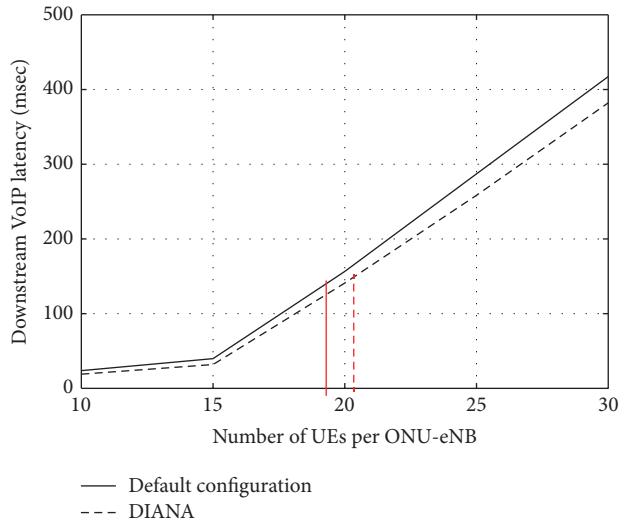

Figure 11: Scenario 2: VoIP downstream latency.

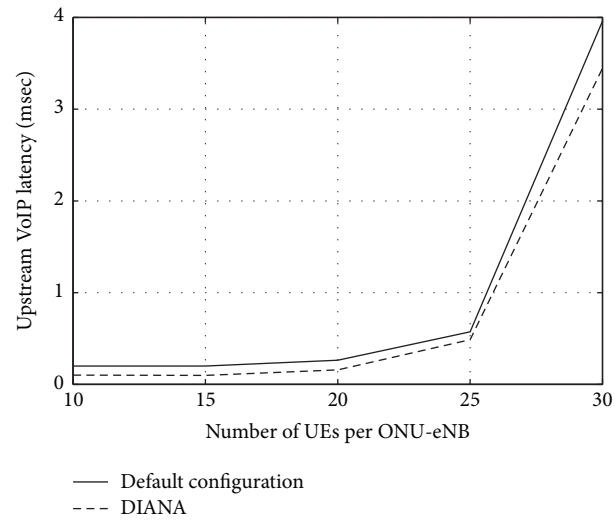

Figure 12: Scenario 2: VoIP upstream latency.

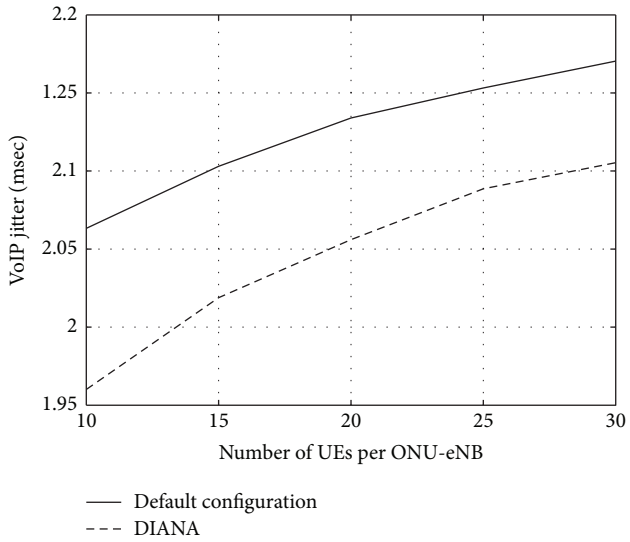

Figure 13: Scenario 1: VoIP jitter.

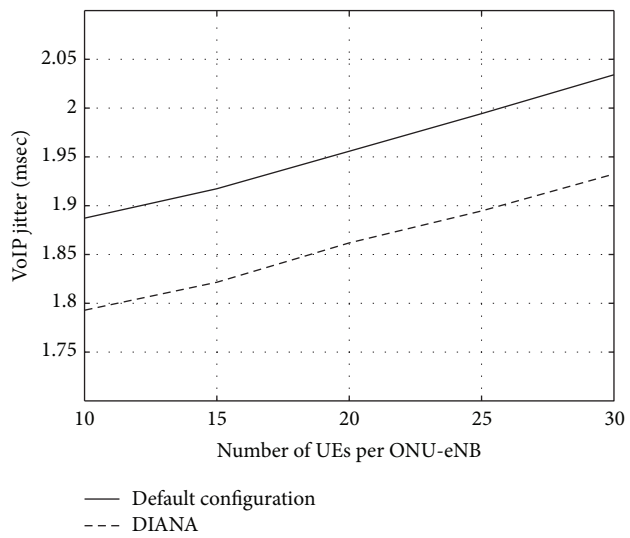

Figure 14: Scenario 2: VoIP jitter.

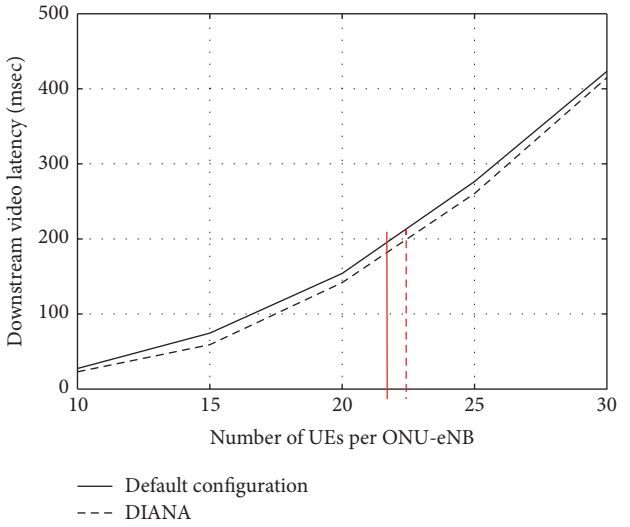

Figure 15: Scenario 1: video downstream latency.

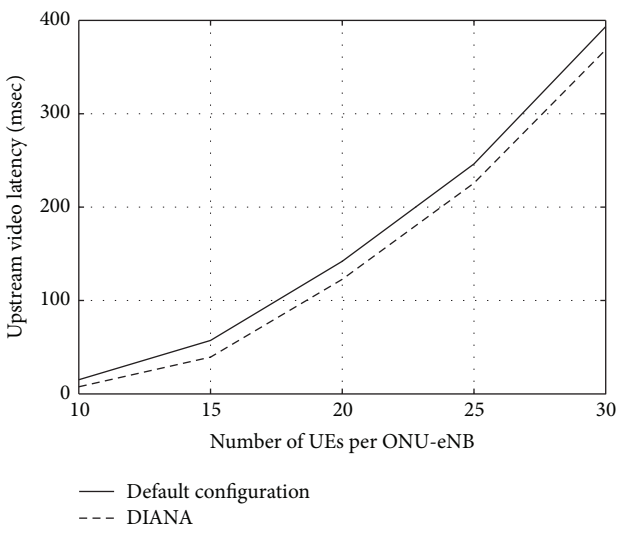

Figure 16: Scenario 1: video upstream latency.

The jitter performance is shown in Figures 13 and 14 for the first and the second scenarios, respectively. Note that these numerical results represent the total average values including both downlink and uplink streams. The quality requirements of jitter imply a latency performance lower than 50 msec. Both scenarios sustain a safe jitter performance. DIANA succeeds in slightly improving the jitter performance compared to the static scheme of about 5%. The measured jitter seems to slightly increase as the number of UEs tends to increase, since more bandwidth requests exist in the network. However, DIANA offers better VoIP performance in total in terms of improved latency and slightly improved jitter.

Figures 15 and 16 show the video performance, in the downlink and uplink directions, respectively, for the first scenario. Once more DIANA presents better performance than the default configuration. The superiority of DIANA is proven by the results of the second scenario as well in Figures 17 and 18, which illustrate the video performance in the downlink and uplink directions, respectively, in scenario 2. The QoS requirement of video in terms of latency is <200 msec. DIANA allows 2 UEs more than the default configuration, a fact that proves that the uplink-downlink configuration adjustment could be beneficial for the network performance, allowing more users to be served with the same network resources.

7. Conclusions

A machine learning framework for adjusting the uplink-downlink configuration of the LTE TDD framing structure was presented in this paper. The framework, called DIANA, was applied in a hybrid optical-wireless network, where the traffic dynamics are unpredictable and bursty. The proposed learning approach is based on knowledge obtained by SDN controllers regarding the uplink and downlink traffic requests

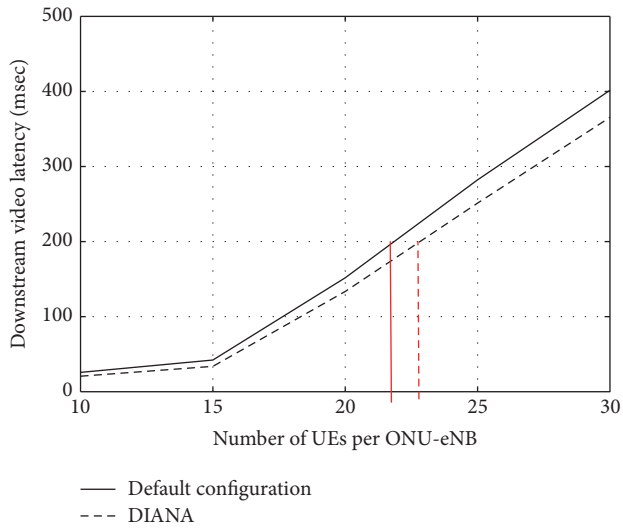

Figure 17: Scenario 2: video downstream latency.

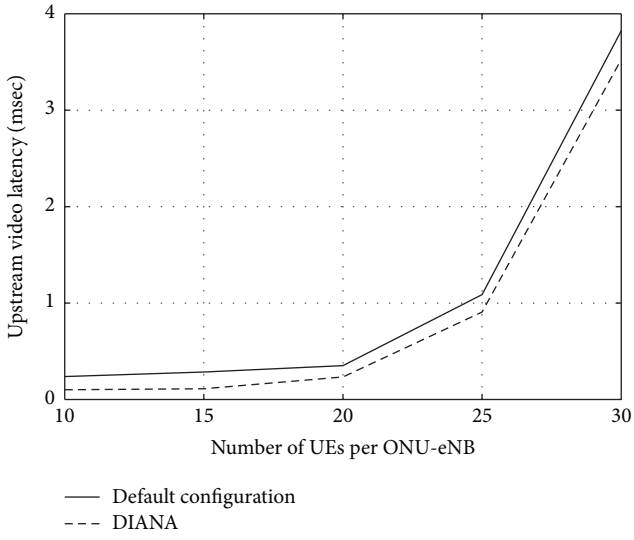

Figure 18: Scenario 2: video upstream latency.

of the mobile end-users. The introduced framework decides the most suitable configuration for the forthcoming TDD frame based on the traffic demands of the previous frames. A probabilistic-based approach ensures the accuracy of the methods by promoting configurations that result in best network performance. The proposed framework was extensively assessed using real traffic traces in terms of VoIP, real-time video, and streaming video. Simulation results indicate the superiority of the traffic-aware framework in any applied channel and traffic parameters. DIANA demonstrated improvements about 40% in terms of average latency, while it demonstrated notable improvements, about 30%, in VoIP and video latency. Our future plans include the expansion of this work in a threefold way. First, we intend to investigate the dynamic adjustment of the LTE frame in hybrid networks, where the optical domain consists of multichannel PONs. Second, we envisage exploring the behaviour of such hybrid optical-wireless networks by considering multiple traffic sources, for example, both mobile end-users and users connected in the optical interfaces. Third, the long-term dependence and the self-similar characteristics of traffic present in access networking will be examined in the light of improving the learning process by making it independent of speed parameters such as W.

Notations

N:	Number of ONU-eNBs
$C = \{c_0, c_1, \ldots, c_7\}$:	The set of the uplink-downlink configuration options
$R = \{r_0, r_1, \ldots, r_7\}$:	Downlink-to-uplink ratio in terms of offered bits
$r_d^i(f)$:	Requested bits in the downlink direction in the i ONU-eNB at frame f
$r_u^i(f)$:	Requested bits in the uplink direction in the i ONU-eNB at frame f
$P^i(f)$:	Ratio probability vector at frame f
$c_s^i(f)$:	Feedback in terms of configuration at frame f
W:	Learning speed parameter
a:	Probability protection parameter.

Conflicts of Interest

The authors declare that there are no conflicts of interest regarding the publication of this paper.

References

[1] E. Wong, "Next-generation broadband access networks and technologies," *Journal of Lightwave Technology*, vol. 30, no. 4, Article ID 6094146, pp. 597–608, 2012.

[2] A. S. Thyagaturu, A. Mercian, M. P. McGarry, M. Reisslein, and W. Kellerer, "Software Defined Optical Networks (SDONs): a comprehensive survey," *IEEE Communications Surveys and Tutorials*, vol. 18, no. 4, pp. 2738–2786, 2016.

[3] O. Gerstel, M. Jinno, A. Lord, and S. J. B. Yoo, "Elastic optical networking: a new dawn for the optical layer?" *IEEE Communications Magazine*, vol. 50, no. 2, pp. S12–S20, 2012.

[4] S. Sun, M. Kadoch, L. Gong, and B. Rong, "Integrating network function virtualization with SDR and SDN for 4G/5G networks," *IEEE Network*, vol. 29, no. 3, pp. 54–59, 2015.

[5] S. Wang, L. Sun, Q. Sun, X. Li, and F. Yang, "Efficient service selection in mobile information systems," *Mobile Information Systems*, vol. 2015, Article ID 949436, 10 pages, 2015.

[6] A. G. Sarigiannidis, M. Iloridou, P. Nicopolitidis et al., "Architectures and bandwidth allocation schemes for hybrid wireless-optical networks," *IEEE Communications Surveys and Tutorials*, vol. 17, no. 1, pp. 427–468, 2015.

[7] G. Shen, R. S. Tucker, and C.-J. Chae, "Fixed mobile convergence architectures for broadband access: Integration of EPON and WiMAX," *IEEE Communications Magazine*, vol. 45, no. 8, pp. 44–50, 2007.

[8] N. Chen, S. Sun, M. Kadoch, and B. Rong, "SDN controlled mmwave massive MIMO hybrid precoding for 5G heterogeneous mobile systems," *Mobile Information Systems*, vol. 2016, Article ID 9767065, 10 pages, 2016.

[9] T. Kamisaka, T. Kuri, and K.-I. Kitayama, "Simultaneous modulation and fiber-optic transmission of 10-Gb/s baseband and 60-GHz-band radio signals on a single wavelength," *IEEE Transactions on Microwave Theory and Techniques*, vol. 49, no. 10, pp. 2013–2017, 2001.

[10] A. Martinez, V. Polo, and J. Marti, "Simultaneous baseband and RF optical modulation scheme for feeding wireless and wireline heterogeneous access networks," *IEEE Transactions on Microwave Theory and Techniques*, vol. 49, no. 10, pp. 2018–2024, 2001.

[11] J. Wu, Z. Zhang, Y. Hong, and Y. Wen, "Cloud radio access network (C-RAN): a primer," *IEEE Network*, vol. 29, no. 1, pp. 35–41, 2015.

[12] S. Sarkar, S. Dixit, and B. Mukherjee, "Hybrid wireless-optical broadband-access network (WOBAN): a review of relevant challenges," *Journal of Lightwave Technology*, vol. 25, no. 11, pp. 3329–3340, 2007.

[13] A. S. Reaz, V. Ramamurthi, M. Tornatore, and B. Mukherjee, "Cloud-Integrated WOBAN: an offloading-enabled architecture for service-oriented access networks," *Computer Networks*, vol. 68, pp. 5–19, 2014.

[14] A. Ahmed and A. Shami, "A new bandwidth allocation algorithm for EPON-WiMAX hybrid access networks," in *Proceedings of the 53rd IEEE Global Communications Conference (GLOBECOM '10)*, USA, December 2010.

[15] M. Giuntini, A. Valenti, F. Matera, and S. Di Bartolo, "Quality of service management in hybrid optical-LTE access networks," in *Proceedings of the Future Network and Mobile Summit (FutureNetw '11)*, June 2011.

[16] W.-T. Shaw, S.-W. Wong, N. Cheng et al., "Hybrid architecture and integrated routing in a scalable optical-wireless access network," *Journal of Lightwave Technology*, vol. 25, no. 11, pp. 3443–3451, 2007.

[17] M. A. Ali, G. Ellinas, H. Erkan, A. Hadjiantonis, and R. Dorsinville, "On the vision of complete fixed-mobile convergence," *Journal of Lightwave Technology*, vol. 28, no. 16, Article ID 5473119, pp. 2343–2357, 2010.

[18] S. Ou, K. Yang, M. P. Farrera, C. Okonkwo, and K. M. Guild, "A control bridge to automate the convergence of passive optical networks and IEEE 802.16 (WiMAX) wireless networks," in *Proceedings of the 5th International Conference on Broadband Communications, Networks, and Systems (BROADNETS '08)*, pp. 514–521, September 2008.

[19] N. Moradpoor, G. Parr, S. McClean, B. Scotney, and G. Owusu, "Hybrid optical and wireless technology integrations for next generation broadband access networks," in *Proceedings of the 12th IFIP/IEEE International Symposium on Integrated Network Management (IM '11)*, pp. 1013–1020, May 2011.

[20] N. Sharma, A. Bansal, and P. Garg, "Generalized OSTBC-based subcarrier intensity-modulated MIMO optical wireless communication system," *International Journal of Communication Systems*, 2016.

[21] J. Liu, H. Guo, H. Nishiyama, H. Ujikawa, K. Suzuki, and N. Kato, "New perspectives on future smart FiWi networks: scalability, reliability, and energy efficiency," *IEEE Communications Surveys and Tutorials*, vol. 18, no. 2, pp. 1045–1072, 2016.

[22] A. Panagiotakis, P. Nicopolitidis, G. I. Papadimitriou, and P. G. Sarigiannidis, "Performance Increase for Highly-Loaded RoF Access Networks," *IEEE Communications Letters*, vol. 19, no. 9, pp. 1628–1631, 2015.

[23] P. Sarigiannidis, M. Louta, G. Papadimitriou, I. Moscholios, A. Boucouvalas, and D. Kleftouris, "Alleviating the high propagation delays in FiWi networks: a prediction-based DBA scheme for 10G-EPON-WiMAX systems," in *Proceedings of the 4th International Workshop on Fiber Optics in Access Networks (FOAN '15)*, pp. 45–50, October 2015.

[24] A. Sarigiannidis and P. Nicopolitidis, "Addressing the interdependence in providing fair and efficient bandwidth distribution in hybrid optical-wireless networks," *International Journal of Communication Systems*, vol. 29, no. 10, pp. 1658–1682, 2016.

[25] P. Sarigiannidis, M. Louta, G. Papadimitriou et al., "A metaheuristic bandwidth allocation scheme for FiWi networks using Ant Colony Optimization," in *Proceedings of the 22nd IEEE Symposium on Communications and Vehicular Technology in the Benelux (SCVT '15)*.

[26] D. Hood and E. Trojer, *Gigabit-Capable Passive Optical Networks*, John Wiley & Sons, Inc., Hoboken, NJ, USA, 2012.

[27] D. Simeonidou, R. Nejabati, and M. P. Channegowda, "Software defined optical networks technology and infrastructure: Enabling software-defined optical network operations," in *Proceedings of the Optical Fiber Communication Conference and Exposition and the National Fiber Optic Engineers Conference (OFC/NFOEC '13)*, March 2013.

[28] Y. Lee and Y. Kim, "A design of 10 Gigabit Capable Passive Optical Network (XG-PON1) architecture based on Software Defined Network (SDN)," in *Proceedings of the International Conference on Information Networking (ICOIN '15)*, pp. 402–404, January 2015.

[29] D. Bojic, E. Sasaki, N. Cvijetic et al., "Advanced wireless and optical technologies for small-cell mobile backhaul with dynamic software-defined management," *IEEE Communications Magazine*, vol. 51, no. 9, pp. 86–93, 2013.

[30] "3GPP: E-UTRA and E-UTRAN Overall Description, 3GPP, March 2012, v10.7.0".

[31] F. Capozzi, G. Piro, L. A. Grieco, G. Boggia, and P. Camarda, "Downlink packet scheduling in LTE cellular networks: key design issues and a survey," *IEEE Communications Surveys and Tutorials*, vol. 15, no. 2, pp. 678–700, 2013.

[32] http://www.mathworks.com/.